

# Unloading deformation during layered excavation for the underground powerhouse of Jinping I Hydropower Station, southwest China

Faquan Wu · Xiuhong Hu · Manfu Gong · Jianyou Liu · Aiwu Ren

Received: 23 April 2009 / Accepted: 12 May 2010 / Published online: 20 July 2010  
© Springer-Verlag 2010

**Abstract** The paper discusses the strong asymmetric deformation and failure of the rock surfaces which have taken place in the 40–75 MPa marble during the excavation for the underground powerhouse and transformer chamber of the Jinping I Hydropower Station, southwest China. The deformation and damage of the rock mass closely relate to the magnitude of the geo-stresses, boundary conditions of the underground caverns, rock properties and the method and sequence of excavation. Ground stress test results show that the maximum principal stress reaches 35.7 MPa in the slope, and the average  $\sigma_1$  intersects with the axis of underground powerhouse at an angle of 28°. Strong displacements had taken place at the sidewalls of the caverns and significant instantaneous uplift deformation of the floor occurred, particularly when the first layer was excavated.

**Keywords** Jinping I Hydropower Station · High ground stress · Layer excavation · Asymmetric unloading deformation

**Résumé** L'article discute de la forte dissymétrie de déformation et de rupture des surfaces rocheuses qui ont eu lieu dans le massif de marbre, présentant une résistance de 40 à 75 MPa, pendant l'excavation réalisée pour l'usine souterraine et la salle des transformateurs de la station

---

F. Wu (✉) · X. Hu · J. Liu · A. Ren  
Engineering Geomechanics Laboratory, Institute of Geology and Geophysics, Chinese Academy of Sciences, P.O. Box 9825, Beijing 100029, People's Republic of China  
e-mail: wufaquan@mail.igcas.ac.cn

M. Gong  
HydroChina Chengdu Engineering Corporation,  
Chengdu 610072, People's Republic of China

hydroélectrique de Jinping I, dans le sud-ouest de la Chine. Les déformations et dommages qui ont affecté la masse rocheuse sont étroitement en rapport avec l'intensité des contraintes in situ, les conditions aux limites relatives aux excavations souterraines, les propriétés des roches, la méthode et la séquence d'excavation. Des mesures de contraintes in situ montrent que la contrainte principale maximale atteint 35,7 MPa dans la pente, sa direction recoupant l'axe de l'usine souterraine suivant un angle de 28°. Des déplacements importants des parements de l'excavation souterraine ont eu lieu ainsi que des déformations instantanées de soulèvement du radier, particulièrement lorsque le premier niveau a été excavé.

**Mots clés** Station hydroélectrique de Jinping I · Etat élevé de contraintes in situ · Excavation par niveau · Déformation de déchargement asymétrique

## Introduction

Jinping I Hydropower Station forms part of the Hydropower Gemini currently being constructed on the Great Jinping River Bend of the Yalong River in Sichuan Province, southwest China. The station will generate electricity from a catchment area of 102,560 km<sup>2</sup>, which will be stored behind a 305 m high concrete arch dam. The reservoir capacity will be 7.76 billion m<sup>3</sup> and will have a mean annual discharge of 1,200 m<sup>3</sup>/s. The installed capacity of the station will be 3,600 MW and the mean annual power generation 16.62 billion kW h (Wu and Qi 2001; Qi et al. 2004; Wu and Wang 2001; Zhong et al. 2006).

The water diversion and power generation system are located in the right bank of the Yalong River (Fig. 1). The

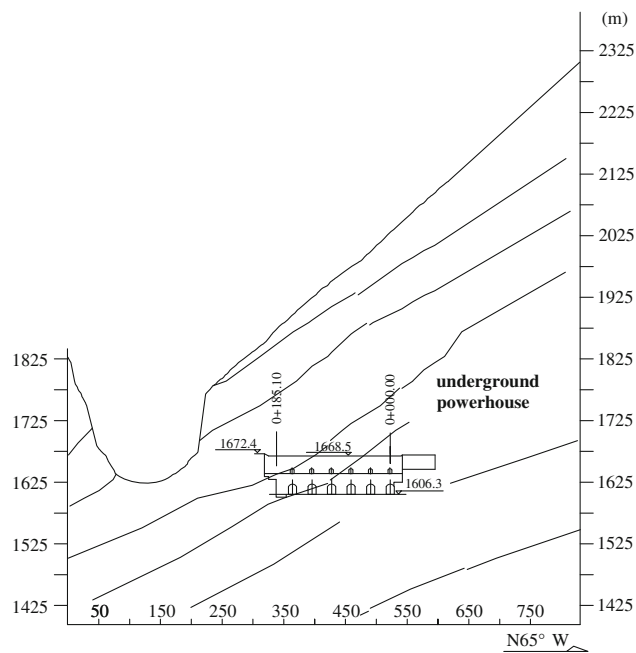


**Fig. 1** Sectional view of the underground powerhouse

main constructions include an underground powerhouse, a transformer chamber and a tailrace surge chamber. These key constructions required large underground caverns, the powerhouse being some  $204.52 \times 25.90 \times 68.83$  m and the main transformer chamber  $201.60 \text{ m} \times 19.30 \text{ m} \times 32.54$  m. Both the powerhouse and main transformer chambers have been designed to have arched roofs and straight walls. The distance between the centers of the two caverns is 67.35 m.

**Regional geological features and ground stress at the dam site**

The Jinping I Hydropower Station is located at the eastern fringe of the tectonic zone known as the Qinghai-Tibet Plateau, where the Indian and Eurasian Plates collide, resulting in high mountains and steep gorges with a topographic height difference of 2,000–3,000 m. In addition to this geological/topographic setting, the presence of the Sichuan Basin to the east means that there are exceptionally high geo-stresses in the area in which the station is being built. The direction of the maximal principal compressive stress changes from SE to SSE in the region of Jinping I Hydropower Station.

The ground stress at the dam site was tested using the aperture and hydraulic fracturing methods (HydroChina Chengdu Engineering Corporation 2007; Seto et al. 1997).

Figure 2 shows the distribution of measured ground stresses around the underground powerhouse. It will be

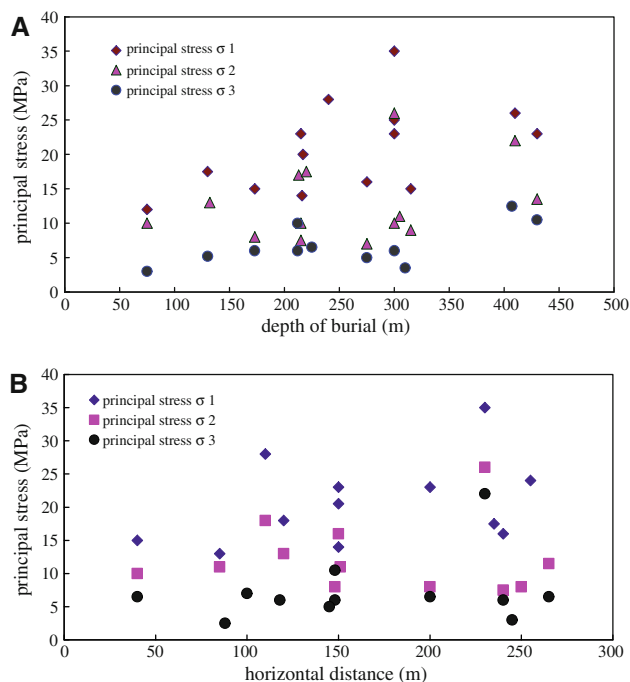


**Fig. 2** Ground stress measured around the underground powerhouse. **a** Principal stress variance versus vertical depth. **b** Principal stress variance versus horizontal distance

noted that  $\sigma_1$  varies significantly with depth and distance from the slope surface,  $\sigma_2$  between 10 and 20 MPa and  $\sigma_3$  between 3 and 12 MPa. As seen in Fig. 1, the main part of the powerhouse is 150 m beneath the slope surface. The measured maximum ground stresses reach  $\sigma_1 = 35.7$  MPa,  $\sigma_2 = 20$  MPa and  $\sigma_3 = 12$  MPa. Figure 3 shows the geometrical relationship between the measured ground stresses and the underground spaces. It is noted that the mean direction of  $\sigma_1$  has a intersection angle of around  $28^\circ$  with the axis of the underground powerhouse and a dip angle of around  $34.5^\circ$  in the cross section of the powerhouse, such that the maximum stress at the powerhouse is asymmetric.

The rocks in which the powerhouse is constructed are mainly thickly bedded marble with uniaxial compressive strengths of around 40–75 MPa. This means that the ratio between the rock strength and maximal ground stress ranges from 1.12 to 2.1.

**Excavation sequence and unloading deformation failure of the underground powerhouse**

In view of the large dimensions of the underground chambers, a layered excavation method was adopted. The powerhouse, with a height of 68.83 m, was divided into 11 excavation levels, each layer being between 5 and 10 m high.

**Fig. 3** Geometrical relationship between measured ground stresses and the underground powerhouse.  
**a** Direction relationship between the measured ground stresses and the axis of the underground powerhouse.  
**b** Dip angle of measured ground stress  $\sigma_1$

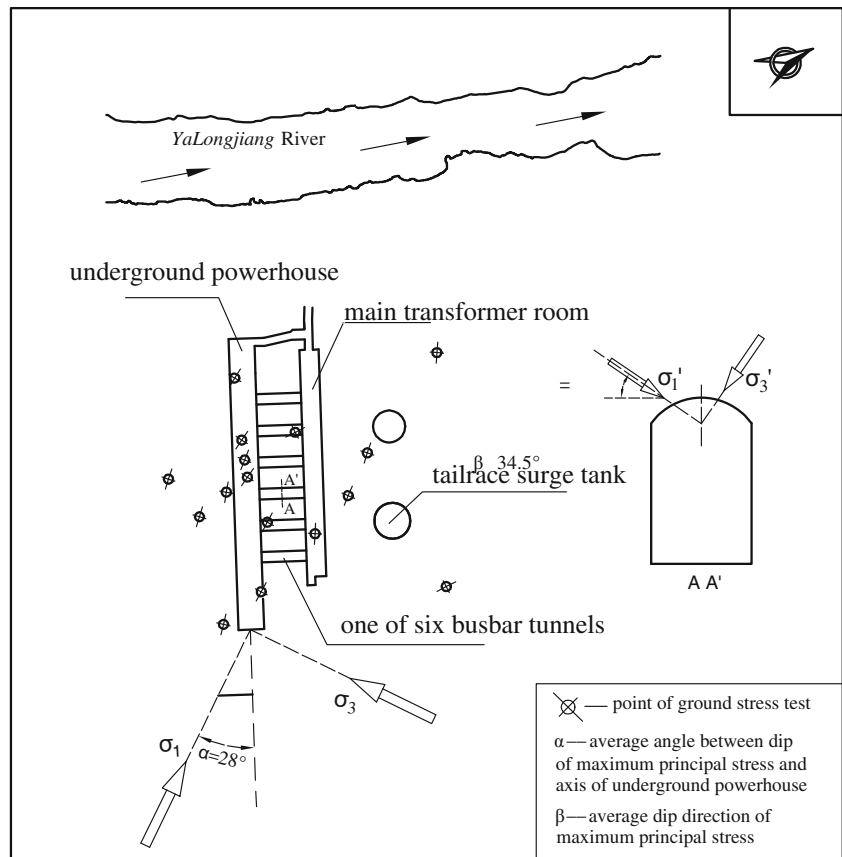


Figure 4 shows the excavation sequence for the underground chambers: 11 layers for the powerhouse and 6 layers for the main transformer chamber. A drill blast method was adopted for the excavation, as it was convenient, efficient and economical, as well as allowing access to deal with geological problems. Although layer excavation using drill and blast ensures that the project proceeds, it results in a progressive disturbance of the stress field and, unless carefully undertaken using pre-splitting, can damage the surrounding rock mass.

Rock stress breakaway is a common phenomenon in hard rock underground engineering. As shown in Fig. 5, most of the breakaways appeared at the right foot of the arch crown when the first layer of the underground powerhouse was excavated. Field records indicate that 15 “flakes” were observed, each with a thickness of 50–500 mm and a broken area of 2–25 m<sup>2</sup>. When the second layer of the powerhouse was excavated, breakaways were observed in only three areas. When the third layer had been completed, they occurred at five positions. Cracks related to the unloading opened by 10–30 mm such that the adjacent rock was disturbed to a depth of some 1 m.

As the excavation continued downwards to the fourth layer, a number of breakaways occurred, notably at the

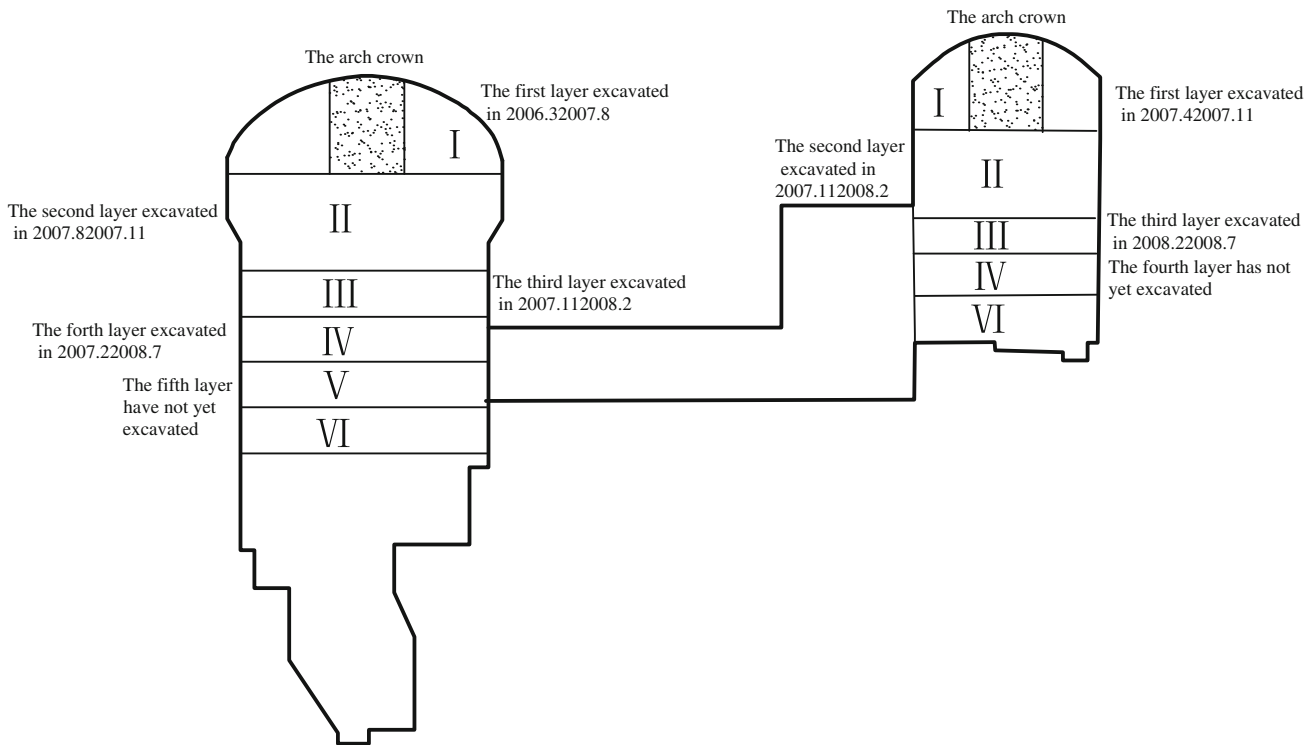
right foot of the arch where it had already been supported by bolts and shotcrete. The shotcrete cracked and broke into slices and the reinforcing bars were bent as shown in Fig. 6 (taken in June 2008).

Figure 7 shows the increase in opening of the cracks against time for three of the largest fractures at the right foot of the arch crown over a 3-month period in 2008. It can be seen that the cracks opened from 10 to 80–100 mm.

#### Deformation of surrounding rock during excavation

In addition to the breakaway fractures, lateral deformation also took place in the rock surrounding the underground chambers. Lateral displacements at varying distances from the face were recorded in boreholes drilled into the side walls and arch of the powerhouse (Fig. 8).

Figure 8 shows monitoring section 2 (0 + 31.7 m) of the underground powerhouse in which extensometers were installed at three positions:  $M_{CF1}$ ,  $M_{CF2}$ ,  $M_{CF3}$ . Figure 9a–c show the curves of displacement versus time in relation to the stages of excavation. It is clear from Fig. 9 that the displacement of the tunnel wall increases gradually and that it is related in part to the stage of the excavation. Up to late July 2008, the displacement at the arch foot had



**Fig. 4** Excavation scheme of the underground powerhouse

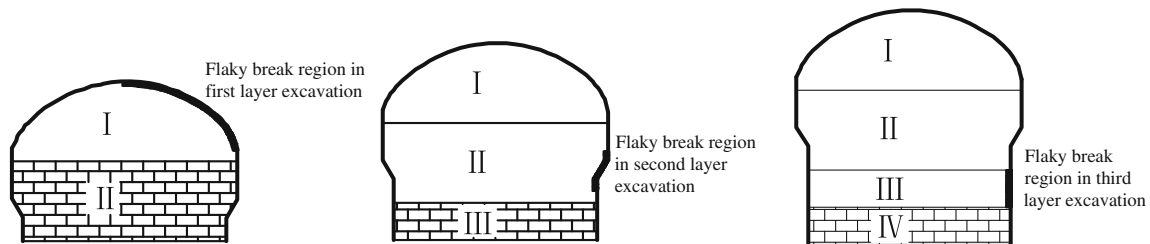


**Fig. 5** Positions of flaky break during the excavation of the underground powerhouse

reached 19.3 mm ( $M_{CF1}$  and  $M_{CF2}$ ), while at the arch curve it was less than 5 mm ( $M_{CF3}$ ). It is of note that the displacement increased rapidly in a short time when the 8 m high fourth layer was excavated.

The deformation in the high and steep sidewalls of the powerhouse along the excavation length was also recorded using extensometers. For convenience of comparison, the same monitoring section (2) is discussed in this paper.

The arrangement of the monitoring instruments and results are shown in Fig. 10. Surprisingly, the data indicate that the displacement of the powerhouse sidewalls is less than that of the main transformer chamber, although the powerhouse is much bigger. The likely explanation is that the transformer chamber is situated between the powerhouse and tailrace surge chamber and hence the deformation is affected by both these openings.

The data for monitoring section 2 also indicate a distinct asymmetry in the deformation, i.e., the displacement at the right arch foot and sidewall is much larger than that on the left side. This is consistent with the rock breakaways at the same position.

Another phenomenon of the deformation is a rise in parts of the cavern floor (Fig. 11).

When the first layer in the powerhouse was excavated, it released a vertical compressive stress of between 10 and 20 MPa. As a consequence of this stress release, heave uplift/rise of the floor of the powerhouse was seen and open, semi-horizontal fractures occurred. Most of the fractures extended for a distance of 3–10 m and had apertures of 5–20 mm. Not surprisingly, there were more open fissures in the central part of the excavation. When the second layer was excavated, some of the stress had

**Fig. 6** Failure of the lining shotcrete at the right foot of the arch crown

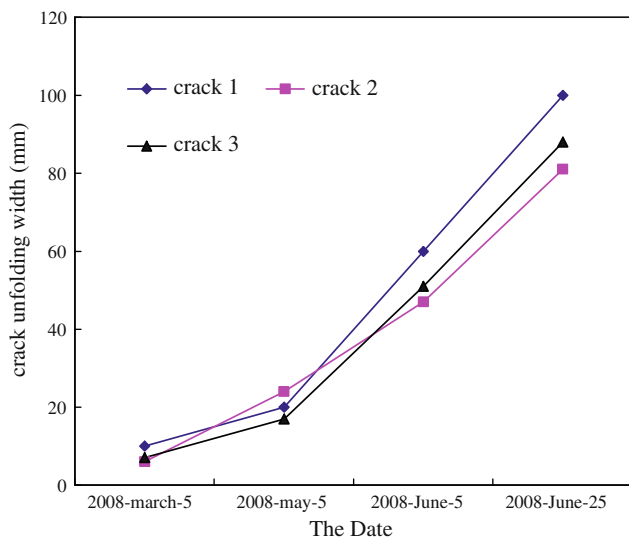


**Fig. 7** Openings of cracks versus time at the right foot of the arch crown

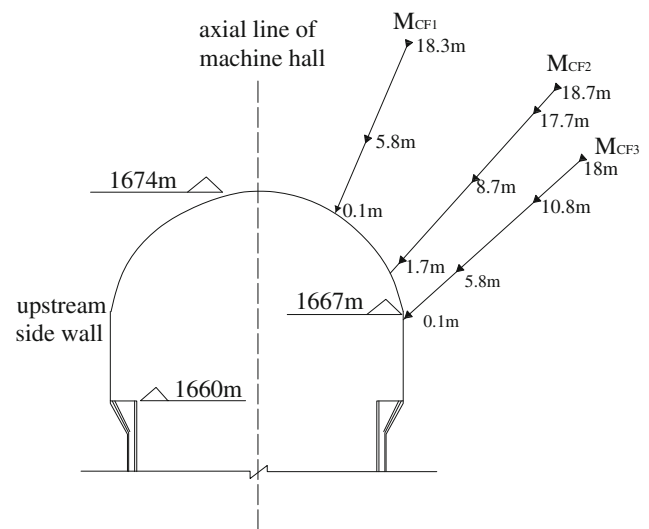


**Fig. 8** Instruments at section 2# of the powerhouse

already been released; hence, the effect was less with subsequent excavation layers (Fig. 11).

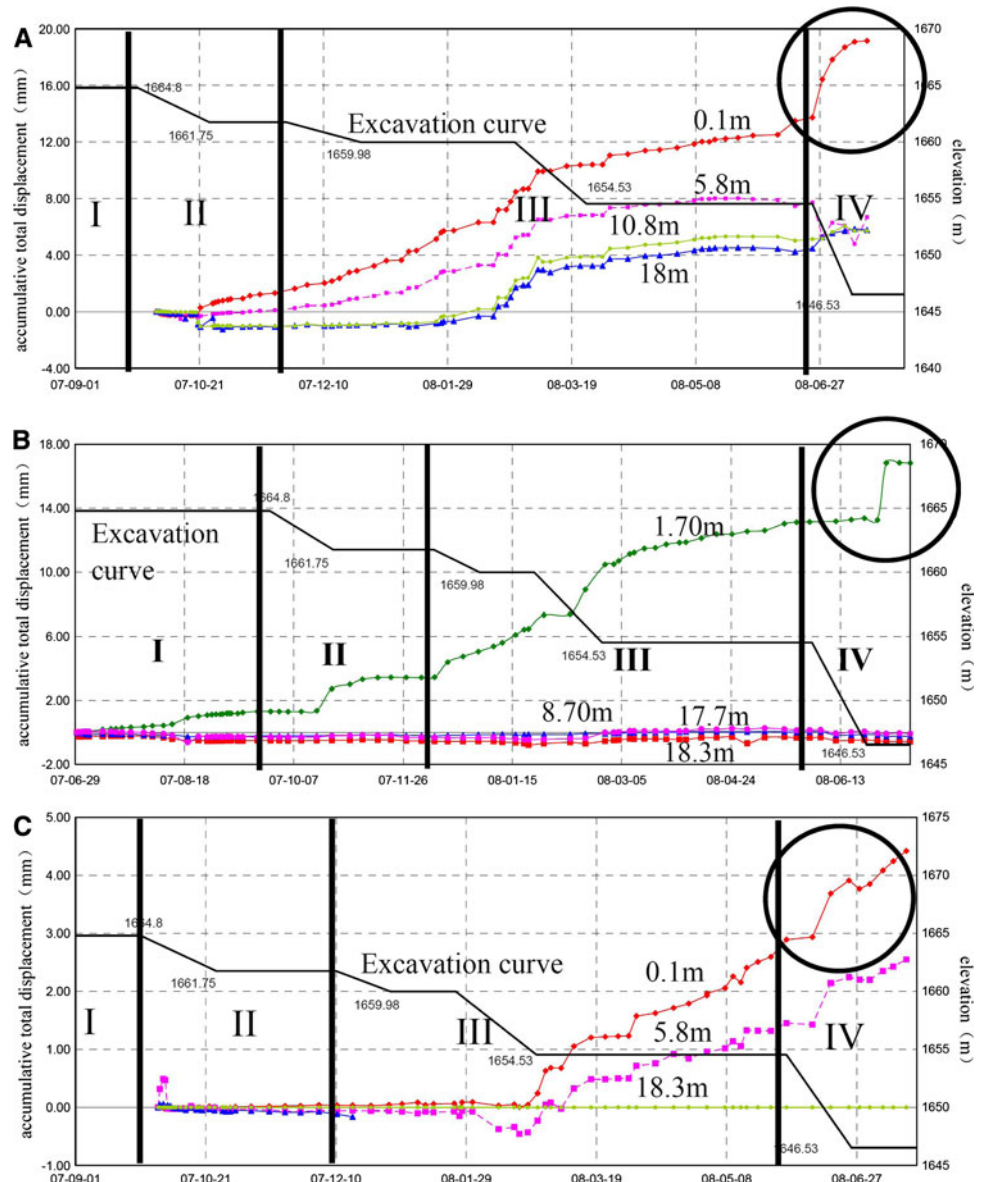
Summarizing, from the above analysis it can be seen that the unloading deformation and failures of the rock at the excavated perimeter of the powerhouse have the following features:

1. Rock breakaways reflect the strong stress concentration caused by excavation, hence they are mainly at one foot of the powerhouse arch and the related

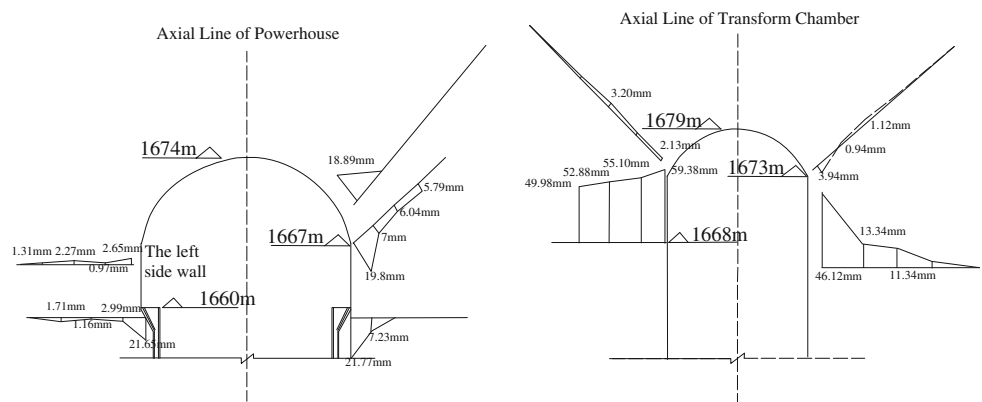
sidewall, indicating the asymmetric nature of the background geo-stress.

2. Unloading deformation of the surrounding rock mass tends to increase in a step-like manner as the individual layers are excavated; the thicker the excavated layer, the larger is the displacement observed.
3. A notable uplift/rise took place when the first layer was excavated as a consequence of the sudden initial unloading of the geo-stress. This effect decreased as the excavation proceeded.

**Fig. 9** Displacement versus time at the right arch of 2# monitoring section



**Fig. 10** Monitoring section 2# for deformation of the powerhouse sidewalls (HydroChina Chengdu Engineering Corporation)



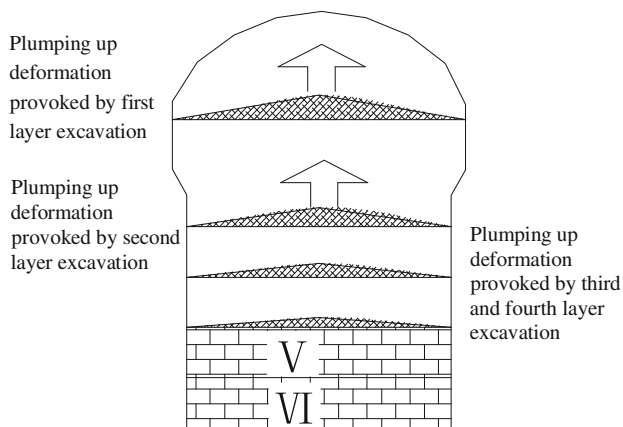


**Fig. 11** Plumping up deformation at the cavern floor of the powerhouse

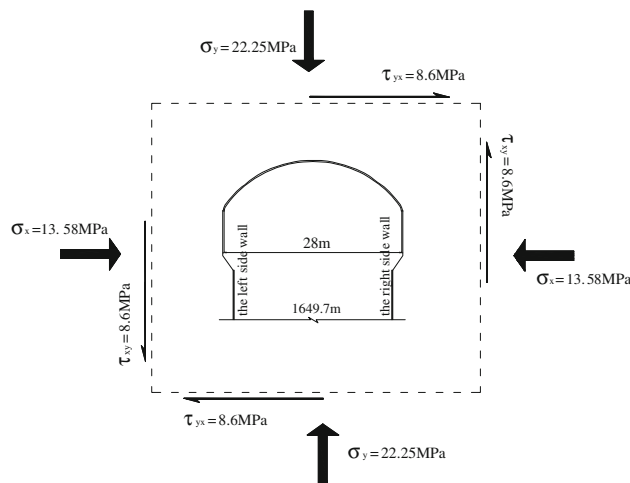


**Fig. 12** Plane stress system on the cross profile of the powerhouse

### Numerical analysis of the unloading deformation

To explain the mechanism of the unloading deformation and failure of the surrounding rock in the underground chambers, a numerical analysis was carried out with the software, FLAC3D, developed by Itasca Corporation.

The stress boundary condition of the calculation model

As seen in Fig. 3, a series of data of in situ geo-stress measurements were taken using the aperture and hydraulic fracturing methods (HydroChina Chengdu Engineering Corporation 2007; Seto et al. 1997). Six sets of stress data from the region of the powerhouse were selected for the numerical calculation; the average values were  $\sigma_1 = 25 \text{ MPa}$  with an attitude of  $SE315^\circ \angle 35^\circ$ ,  $\sigma_2 = 15 \text{ MPa}$  and  $NE87^\circ \angle 45^\circ$ , and  $\sigma_3 = 9 \text{ MPa}$  and  $NE205^\circ \angle 25^\circ$ . Through stress coordinate conversion, the plane stress system on the cross profile of the powerhouse ( $z$  axis vertical and  $x$  axis horizontal) was calculated as  $\sigma_z = 22.25 \text{ MPa}$ ,  $\sigma_x = 13.5 \text{ MPa}$ , and  $\tau_{zx} = \tau_{xz} = 8.6 \text{ MPa}$  (Fig. 12).

As seen, the powerhouse is in an asymmetric state of stress. Qualitative analysis based on the elastic solution of round holes infers that there should be a compressive stress-decrease region (labeled 1 in Fig. 13) and two compressive stress-concentrated regions (2 and 3). This is the cause of the asymmetric distribution of forces and deformation and hence the failure phenomena of the rock surrounding the powerhouse.

Numerical analysis of underground powerhouse under layering excavation

Numerical simulation of the excavation for the powerhouse and transformer chamber was carried out in the following

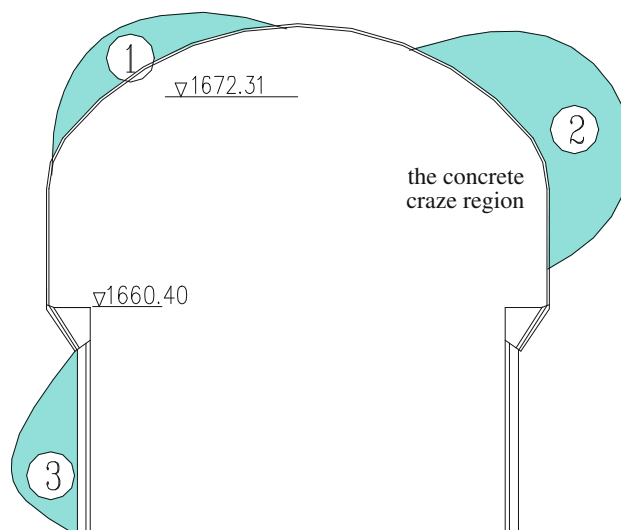


**Fig. 13** Stress concentration regions provoked by asymmetrical pressure

five steps, which are consistent with the six steps of the real excavation process.

- Step 1: first and second layer of the powerhouse and the first layer of the transformer chamber;
- Step 2: third layer of the powerhouse and the second layer of the transformer chamber;
- Step 3: third layer of the powerhouse and the third layer of the transformer chamber;
- Step 4: fourth layer of the powerhouse and the third layer of the transformer chamber;
- Step 5: fifth layer of the powerhouse and the fourth layer of the transformer chamber;
- Step 6: sixth layer of the powerhouse and the fourth layer of the transformer chamber.

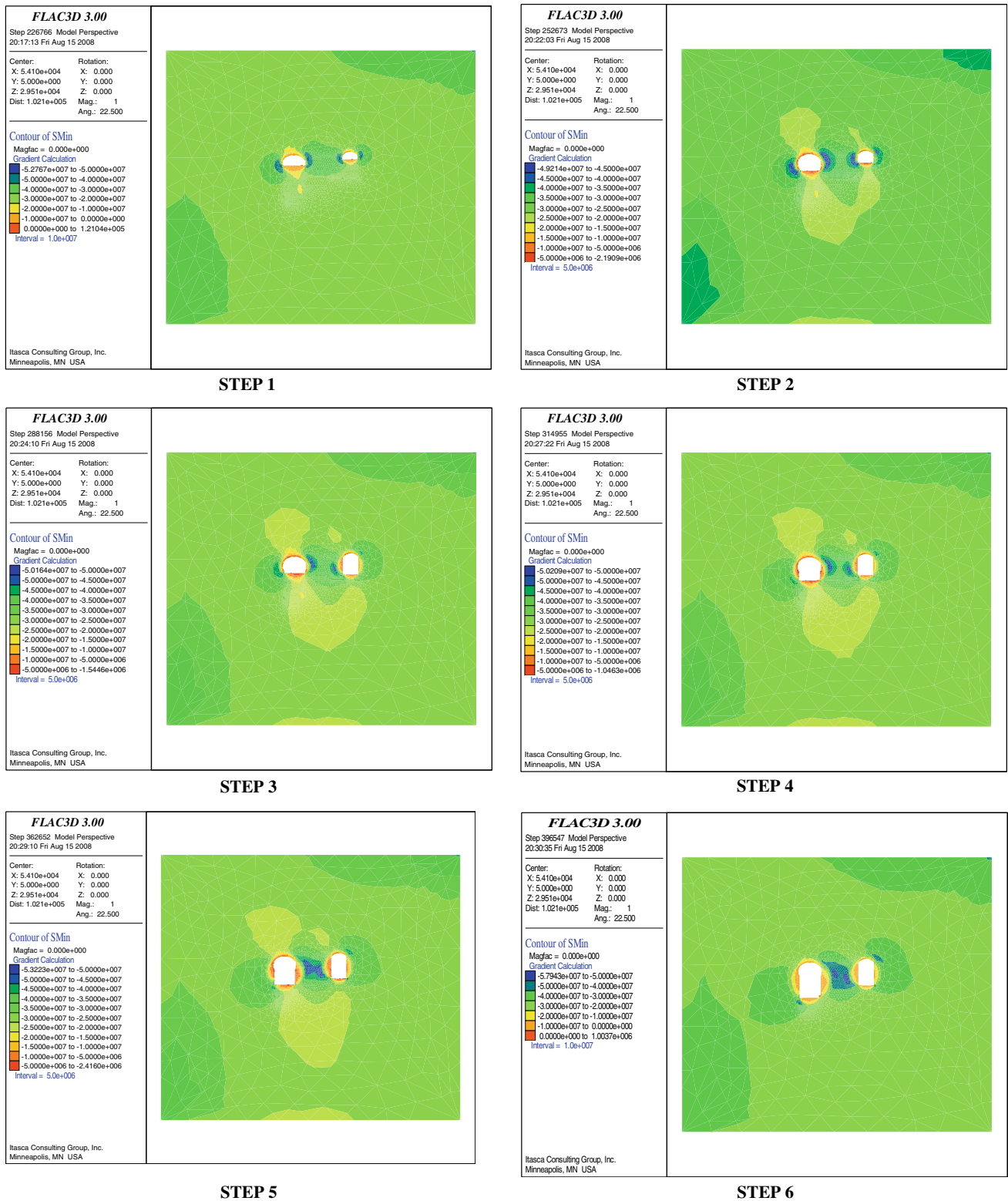


**Fig. 14** The maximum principal stress distribution after excavation

The calculated results of maximum principal stress distribution for the five excavation steps are shown in Fig. 14a–f. From the contoured diagrams it can be seen that:

1. following excavation, the rearranged stress concentrates at two locations (the right foot of the arch crown and the left foot of the sidewall) because of the asymmetric background stress state;



2. the magnitude of the rearranged stresses at the right foot of the arch crown increased to 50–52.7 MPa; hence, the rock at the corner was more easily damaged. After the first step of the excavation, the stress at the corner suddenly increased by 22.7–30 MPa and then only very little in the following five steps. This is the reason why the perimeter rocks break at the first step of the excavation, but this decreases as the excavation continues;
3. the stress is usually about 20 MPa lower than the background value at the foot and left curve of the arch crown. This appears to be the explanation for the rebound deformation at these positions;
4. similarly, as the height of the sidewall increases with the excavation, the stress at the sidewalls decreases by about 22.5 MPa, close to the background value of 25 MPa. This explains the rebound deformation of the sidewalls;
5. the stress in the region between the two chambers increases to 30–58 MPa. However, there will be two layers of tunnels passing through this region, each with six tunnels of 8–16.5 m diameter, with the axial spacing between the two layers being only 29 m. This may bring about serious problems for the construction of the tunnels because of the high background stress in this region.

### Concluding remarks

The case study discusses a series of engineering geological and rock mechanics issues when chambers are excavated in areas of high geo-stress. In summary:

1. The high geo-stresses, hard rock and large scale underground chambers are the main reasons for the strong unloading deformation of the rocks surrounding the powerhouse at Jinping I hydroelectric power station. The excavation leads to high stress concentrations; the maximum principal stress is higher than 50 MPa such that rock mass breakaways occur.
2. The failure mode of the rock mass is mainly breakaways: a kind of flaky rock burst. In addition, stress relief uplift of the excavated floor occurs, being greatest in the middle of the open space and decreasing as the excavation progresses.
3. Asymmetric background stress results in the breakaways being concentrated at the right foot of the arch crown and the right sidewall of the powerhouse.
4. The first step of the excavation resulted in a notable rebound, but the effect decreased as the excavation proceeded.

**Acknowledgments** The authors are grateful for the financial support from Chinese Academy of Sciences under grant of KZCX2-YW-109-2.

### References

- HydroChina Chengdu Engineering Corporation (2007) Report of selecting dam site for Jinping first stage hydropower station, 4 Engineering geological condition (in Chinese)
- Qi S, Wu F, Yan F, Lan H (2004) Mechanism of deep cracks in the left bank slope of Jinping first stage hydropower station. *Eng Geol* 73:129–144
- Seto M, Utagawa M, Katsuyama K, Nag DK, Vutukuri VS (1997) In situ stress determination by acoustic emission technique. *Int J Rock Mech Min Sci* 34:3–4 (paper no. 281)
- Wu F, Qi S (2001) Report of numerical simulation study on mechanism of deep cracks as well as their influence to stability and deformation of the left abutment slope of Jinping first stage hydropower station (in Chinese)
- Wu F, Wang S (2001) A stress–strain relation for jointed rock masses. *Int J Rock Mech Min Sci* 38(4):591–598
- Zhong D-H, Li M-C, Song L-G, Wang G (2006) Enhanced NURBS modeling and visualization for large 3D geoenvironmental applications: an example from the Jinping first-level hydropower engineering project, China. *Comput Geosci* 32:1270–1282